Quasars at Very Low-Frequencies: Cosmic evolution and the origins of their radio emission.

6th CSSGPS workshop
virtual meeting
11 May, 2021

Edwin Retana-Montenegro, UKZN

Outline:

- Open questions and challenges
- New opportunites offered by new radio-telescopes: LOFAR
- Cosmic Evolution of Quasars
- Origins of radio-emission in Quasars
- Take home messages

Introduction: Context

- First quasar discovered is a strong radio source (3C273).
- But, not all quasars are bright in the radio.
- Radio-loud/Radio-quiet dichotonomy.

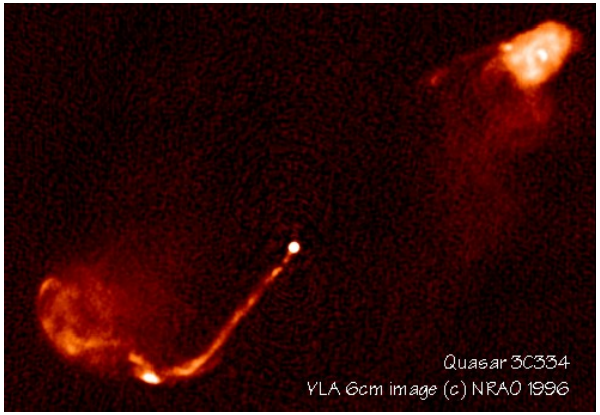

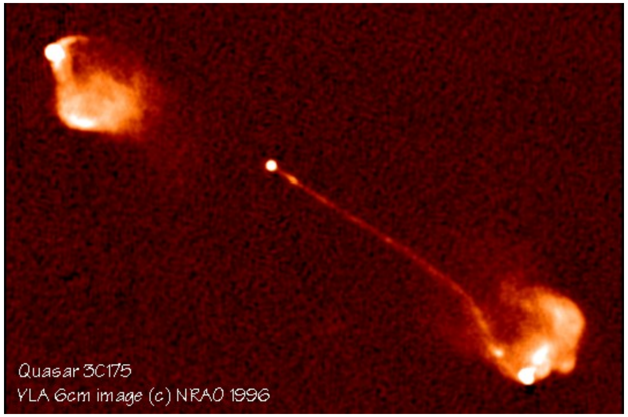

- Cosmic evolution of radio quasars?
- Why some quasars have radio jets?

New opportunities with deep LOFAR observations

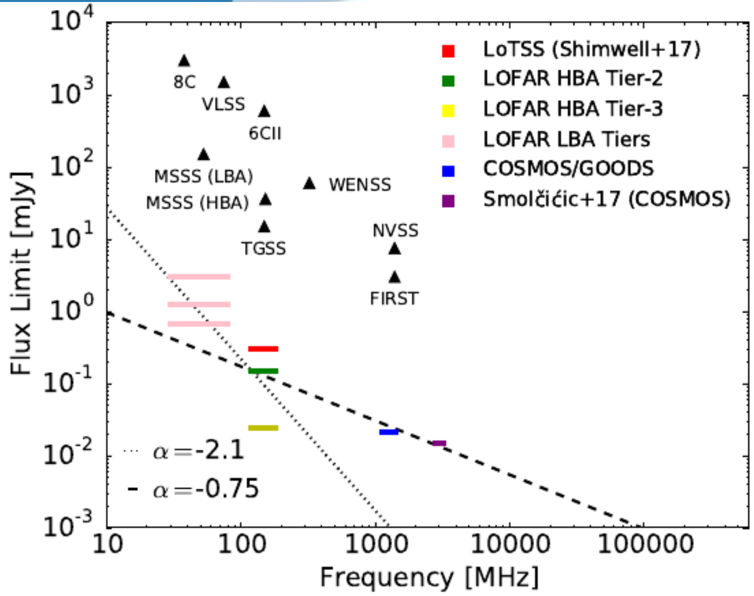

- To explore a relatively new parameter space to look for quasars.
- To detect the radio emission of non "radio-loud" quasars with deep LOFAR observations.

Retana-Montenegro et al. 2018 A&A, 620, A74 .

New opportunities with deep LOFAR observations

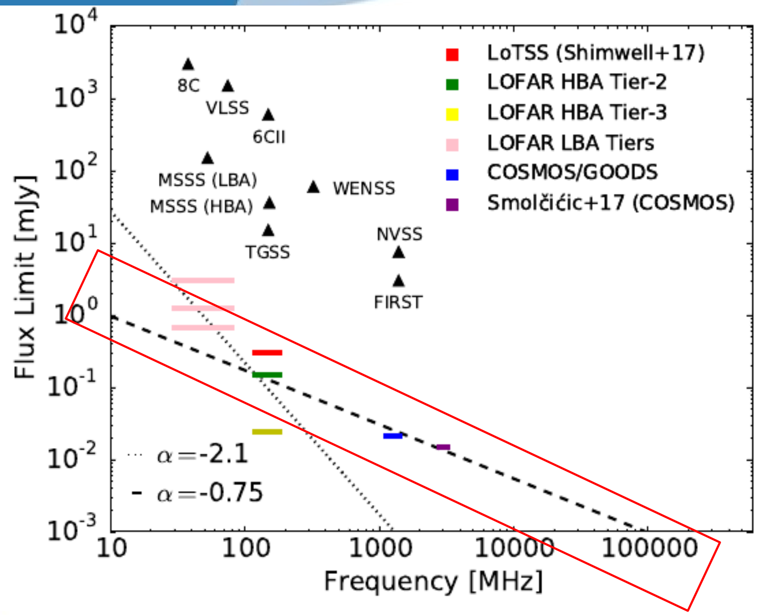

- To explore a relatively new parameter space to look for quasars.
- To detect the radio emission of non "radio-loud" quasars with deep LOFAR observations.

Retana-Montenegro et al. 2018 A&A, 620, A74 .

New opportunities with deep LOFAR observations

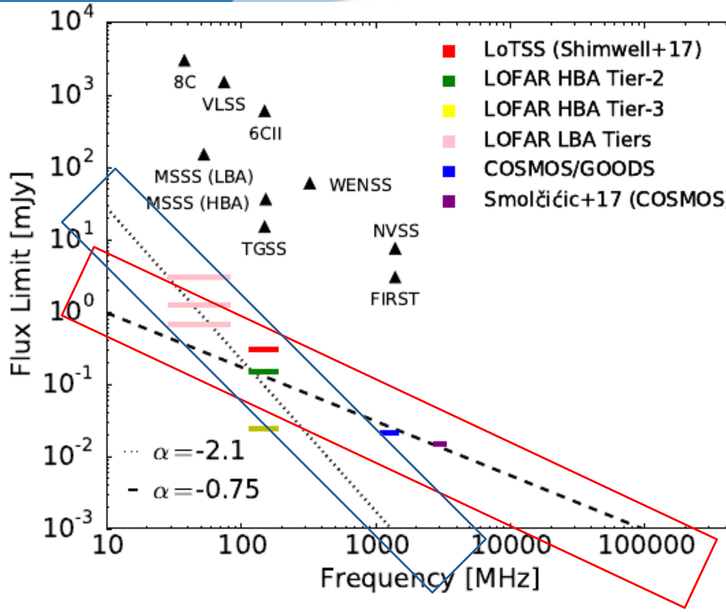

- To explore a relatively new parameter space to look for quasars.
- To detect the radio emission of non "radio-loud" quasars with deep LOFAR observations.

Retana-Montenegro et al. 2020 A&A, 636, A12 .

New opportunities with deep LOFAR observations

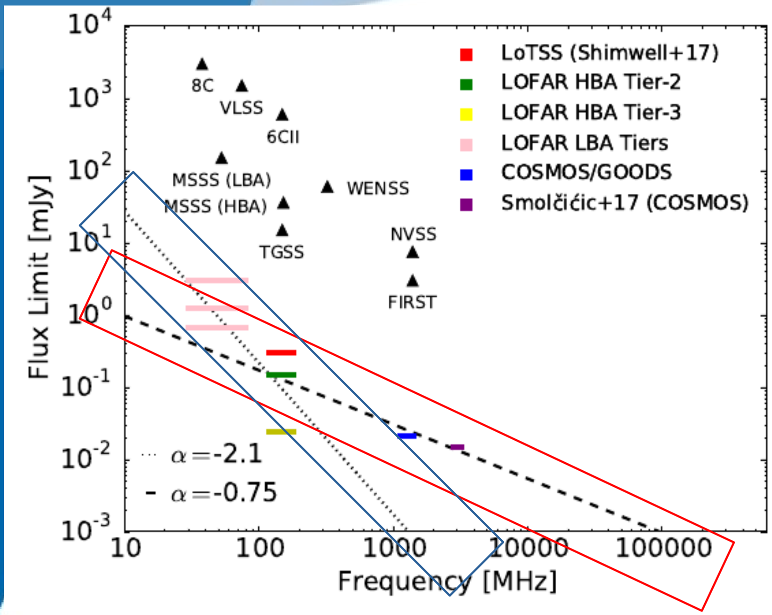

- To explore a relatively new parameter space to look for quasars.
- To detect the radio emission of non “radio-loud” quasars with deep LOFAR observations.

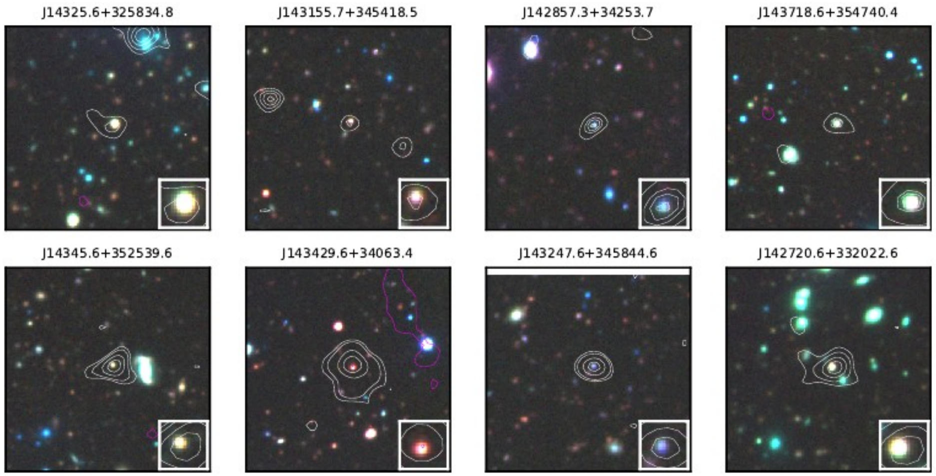

Retana-Montenegro et al. 2020 A&A, 636, A12 .

Part 1: Cosmic Evolution of Radio-Selected Quasars

Deep 150MHz LOFAR Observations of the Boötes field

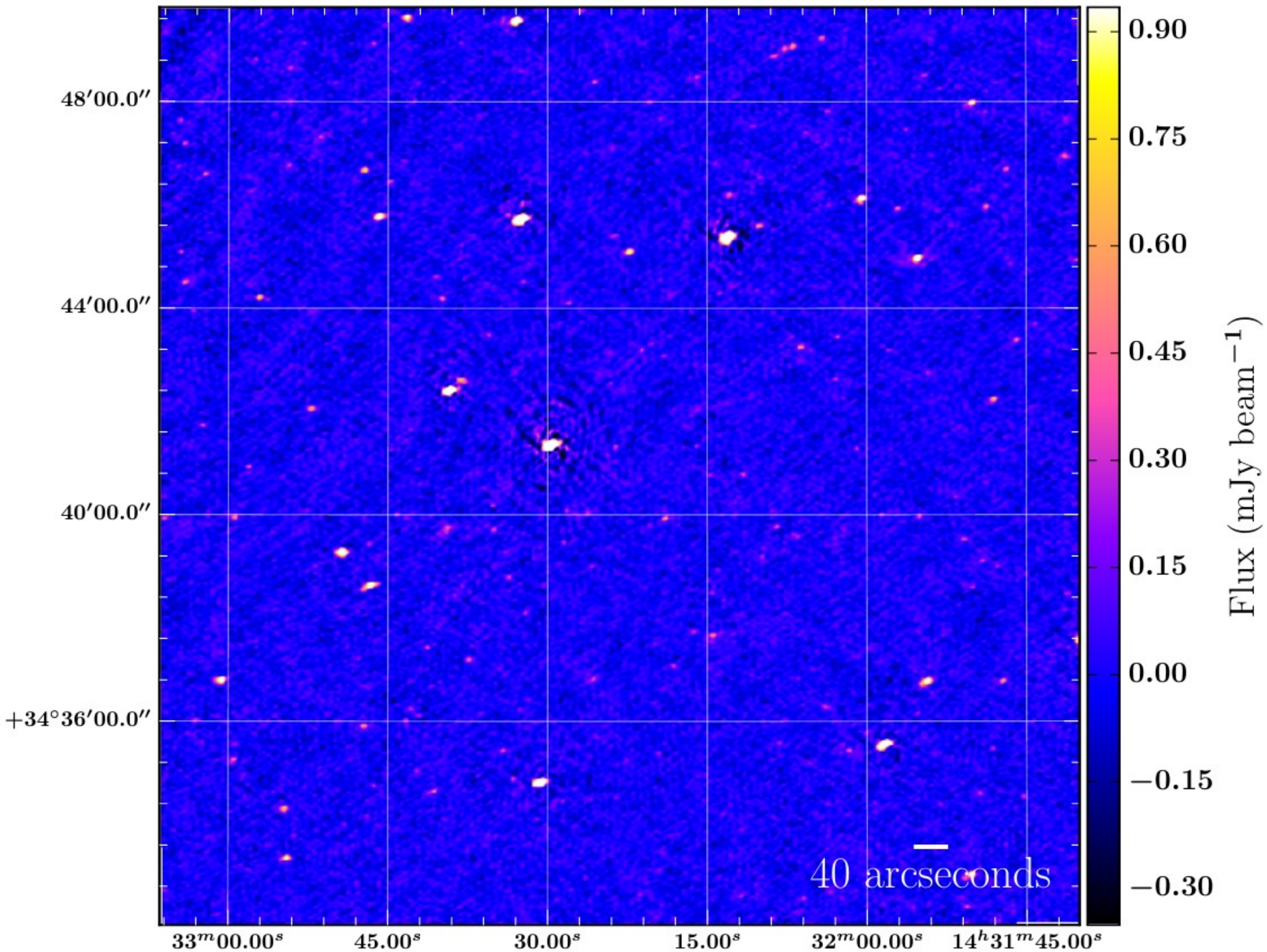

Central region

- 55 hours of observations
- Central rms: ~55 μJy/beam
- Total mosaic area is 20 sq. deg.
- Boötes field is 9.3 sq. deg.
- Large wealth of data: (X-Ray,UV/optical, infrared, radio).
- Spitzer, Hershel, WISE
- WSRT, VLA, LOFAR
- Spectroscopy (AGES, SDSS)

RMS map:

Boötes

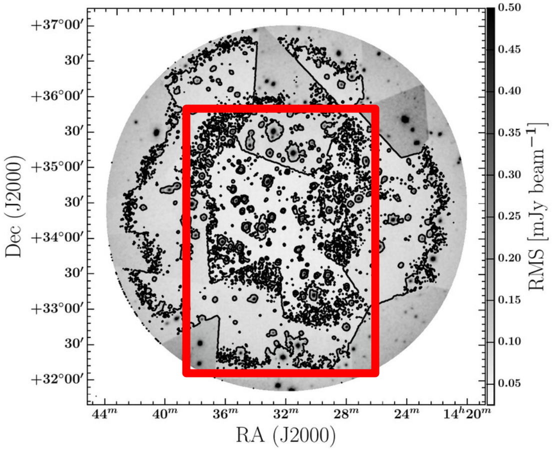

Retana-Montenegro et al. 2018 A&A, 620, A74 .

SMBH downsizing and Color confusion of quasars and stars

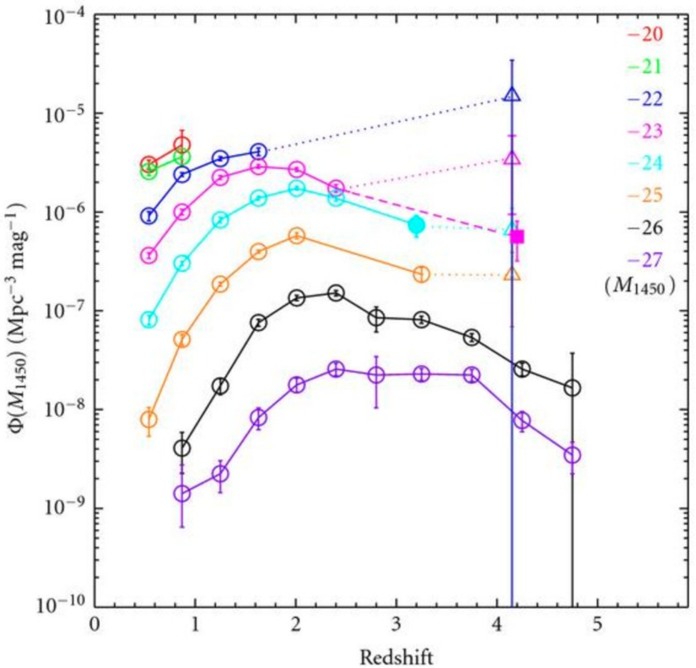

Ikeda et al. 2011.

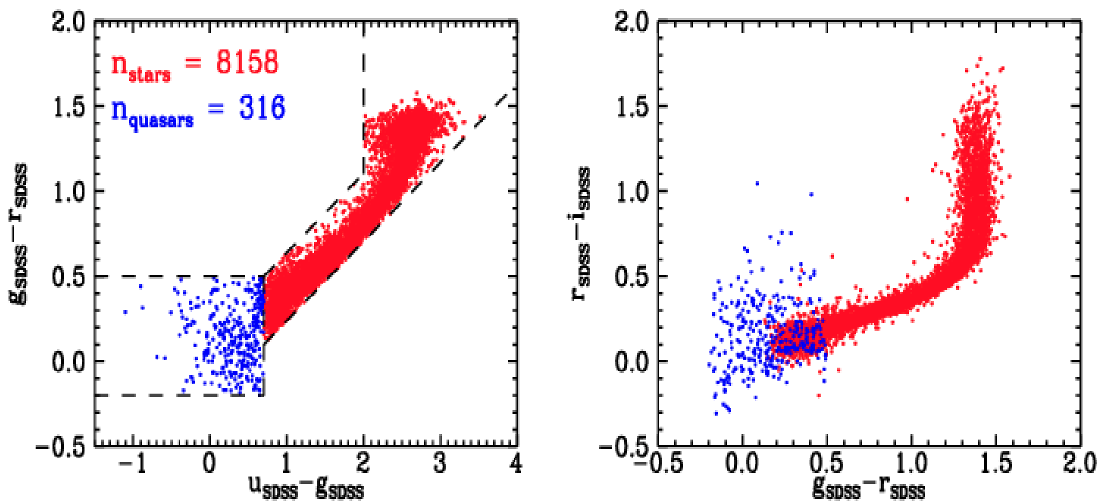

Liu et al. 2015.

- **Black** contours are the quasar training sample.

Selection of Radio-Selected Quasars (RSQs)

Colors used as input for the ML methods

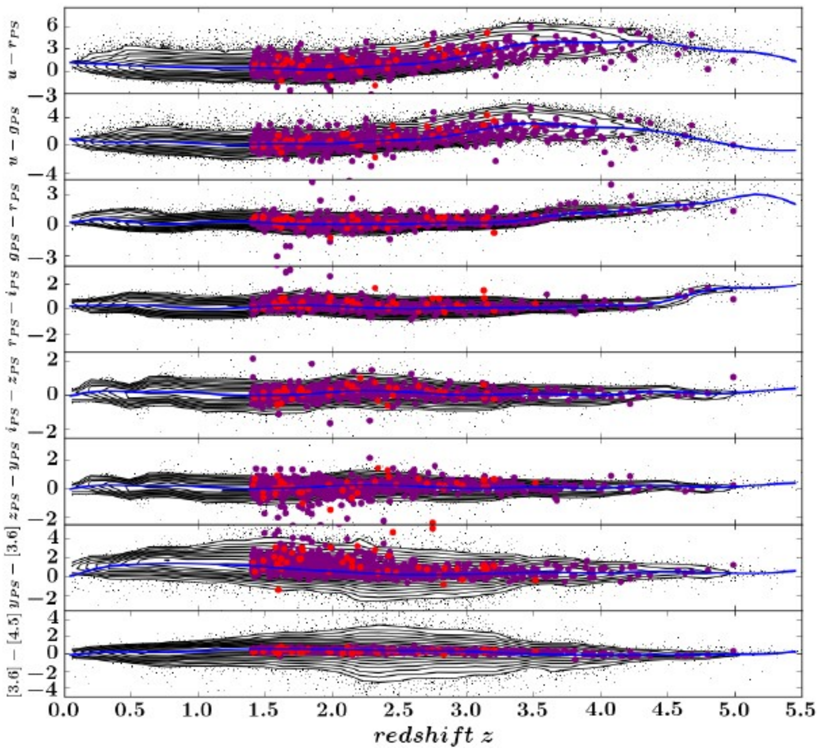

- **Black** contours are the quasar training sample.
- **Purple** points are spectroscopic quasars.
- Red points are the photometric quasars.

- Create a catalog containing the highest number of spectroscopic quasars with optical+mid-infrared photometry (Million Quasars catalog, Flesch+15).

SDSS (u)+ PanStarrs (g,r,i,z,y)+Spitzer-IRAC (3.6µm,4.5µm). + or WISE (W1, W2)

- Use the catalog as a training sample for machine-learning (ML) algorithms (RF+SVM+BA).
- Radio-Detection is required to eliminate stellar contaminants.
- Photometric redshifts assigned using ML.
- Final sample: spectroscopic (47)+photometric (83) quasars.

Retana-Montenegro et al. 2020 A&A, 636, 12.

Luminosity function of RSQs

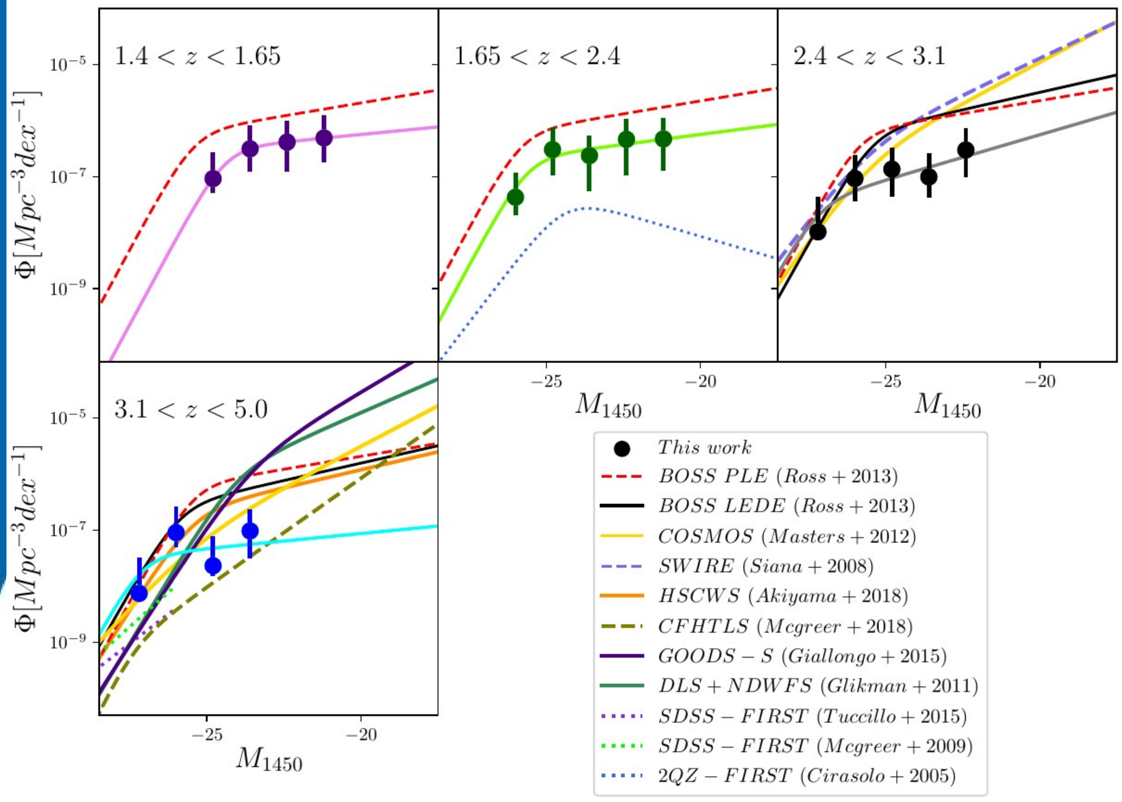

- **Double Power-Law**
- Range:
- -28 <M1450< -22; 1.4<z<5.0
- PLE model for z<2.4
- LEDE model for z>2.4

- **Fixed:**
- **Bright-end slope, β=-3.55**
- **k1,k2,c1,c2** (Ross+13).
- **Determined:**
- **Faint-end slope:**
- α=-1.15 for z<2.4; α=-1.26 for z>2.4;
- **Break Magnitude**
- M1450~-21.2 for z<2.4**;**
- M1450~-26.5 for z>2.4**;**

Retana-Montenegro et al. 2020, A&A, 636, A12.

Spatial density of RSQs (M1450<-22)

$$\rho\,(<M_{1450}\,,z\,) = \int_{-\infty}^{M_{1450}} \Phi\,(\,M_{1450}\,,\,z\,)\,dM$$

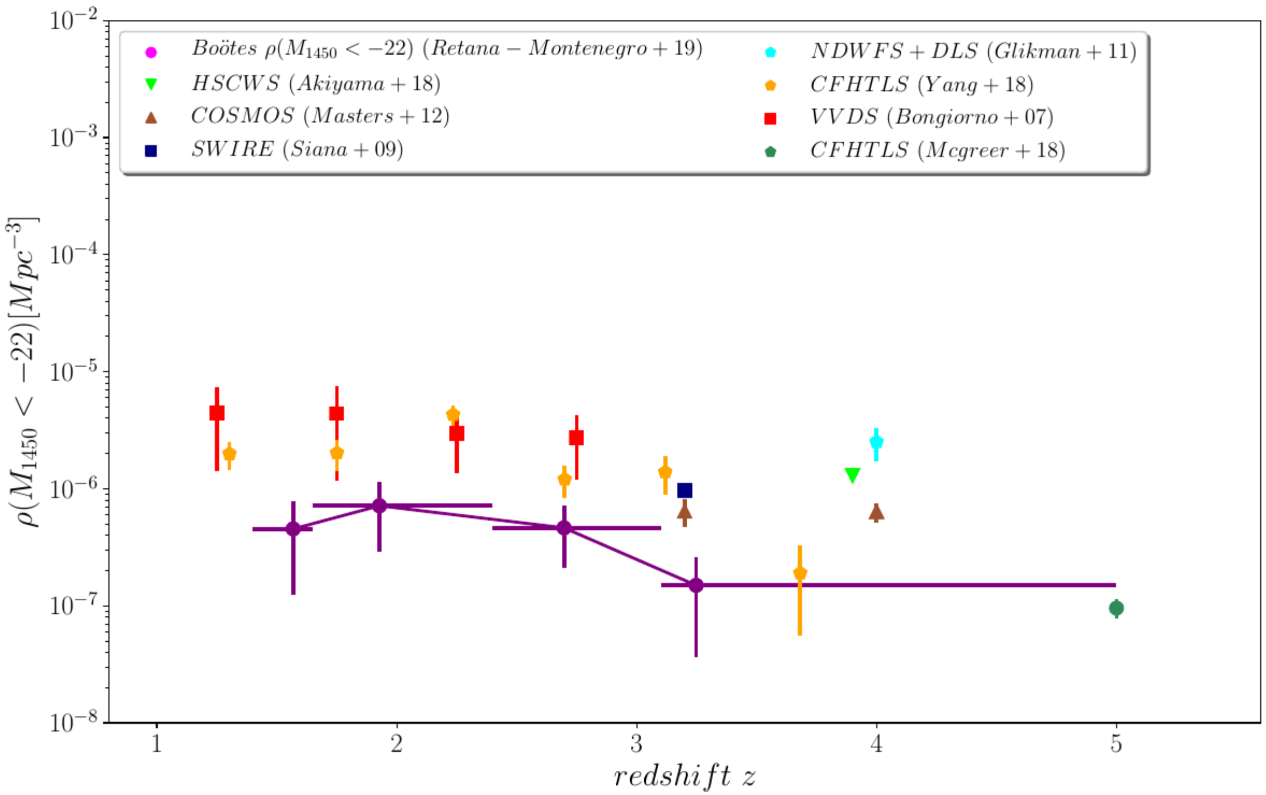

Retana-Montenegro et al. 2020, A&A, 636, A12.

Spatial density of RSQs (M_{1450}<-22)

$$\rho(< M_{1450}, z) = \int_{-\infty}^{M_{1450}} \Phi(M_{1450}, z)\, dM$$

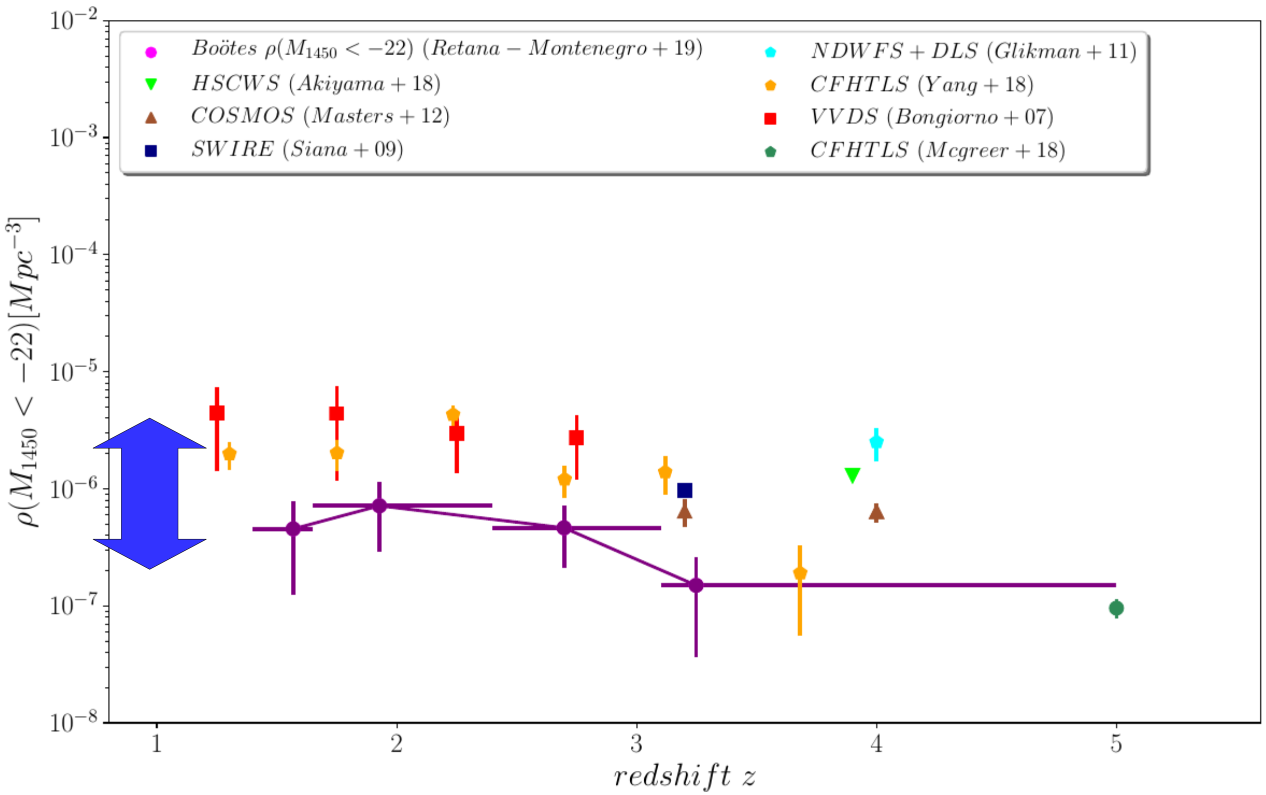

Retana-Montenegro et al. 2020, A&A, 636, A12.

Spatial density of RSQs (M_{1450}<-22)

$$\rho\,(<M_{1450}\,,z\,)=\int_{-\infty}^{M_{1450}}\Phi\,(\,M_{1450}\,,\,z\,)\;dM$$

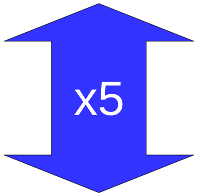

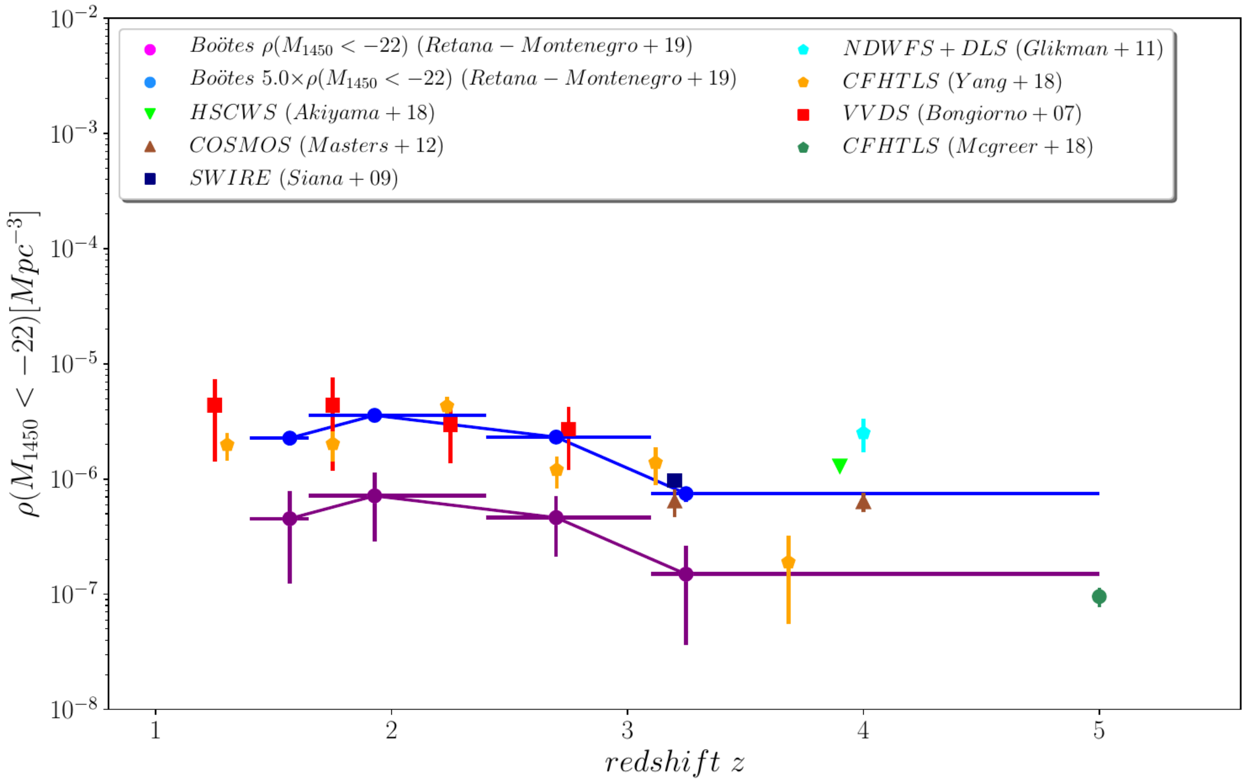

Retana-Montenegro et al. 2020 A&A, 636, A12.

Spatial density normalized to z~2 value

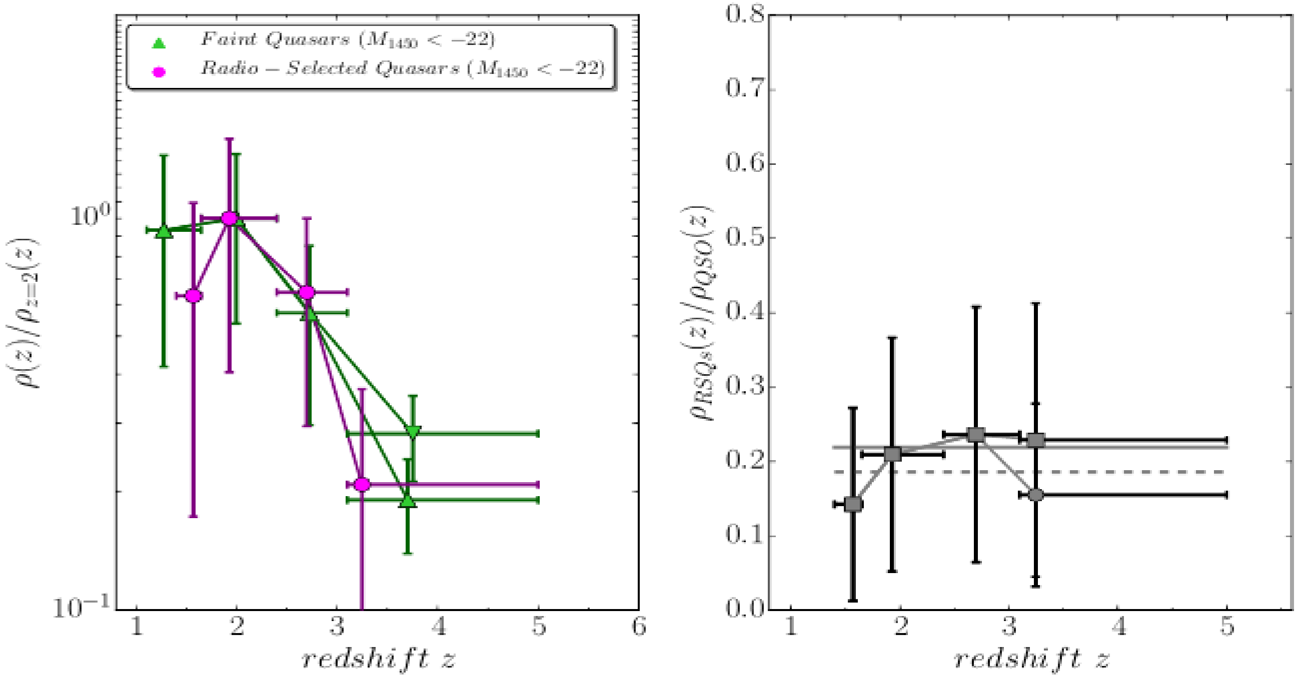

Fraction: ~20%

- *Right:* Upward (downward) triangle excludes (includes) Glikman+11 and Akiyama+18.
- *Left:* Solid line excludes the aforementioned works, dashed line includes them.

Retana-Montenegro et al. 2020 A&A, 636, A12.

Part 2: Origins of radio-emission in quasars

Radio-emission in radio-quiet (radio-undetected) quasars

- Origins of radio-emission in radio-undetected quasars is still under debate.
- Non-thermal component by small-scale radio jets with a kinetic power that is significanly lower than those of RLQs (Miller+93).
- Supported by VLBI observations of RQQs (Herrera-Ruiz+06).
- Thermal component by star-formation processes in the host galaxies (Kimball+11, Bonzini+15)
- Other hypotheses include: magnetically heated accreation disk corona and AGN winds (Laor+08; Zakamska+14).

Retana-Montenegro et al. 2021 A&A, submitted.

Image Stacking (Radio+Infrared)

LOFAR@150MHz

WSRT@1400MHz

VLA@325MHz, 3GHz

Radio

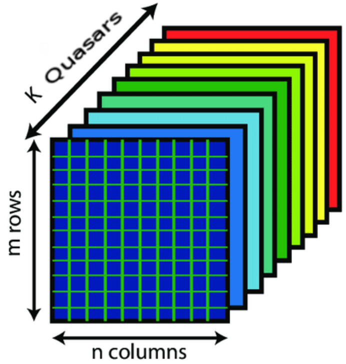

Stacking according to the median
Noise maps using as weights
Sample: 1500 spec quasars with
~230 detected by LOFAR.

Infrared

Spitzer@Mid-IR

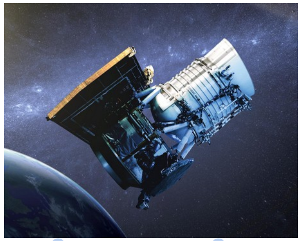

WISE@Mid-IR

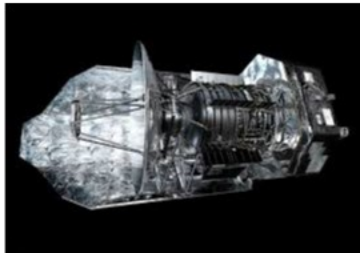

Herschel@FIR

Image Stacking Results (Radio)

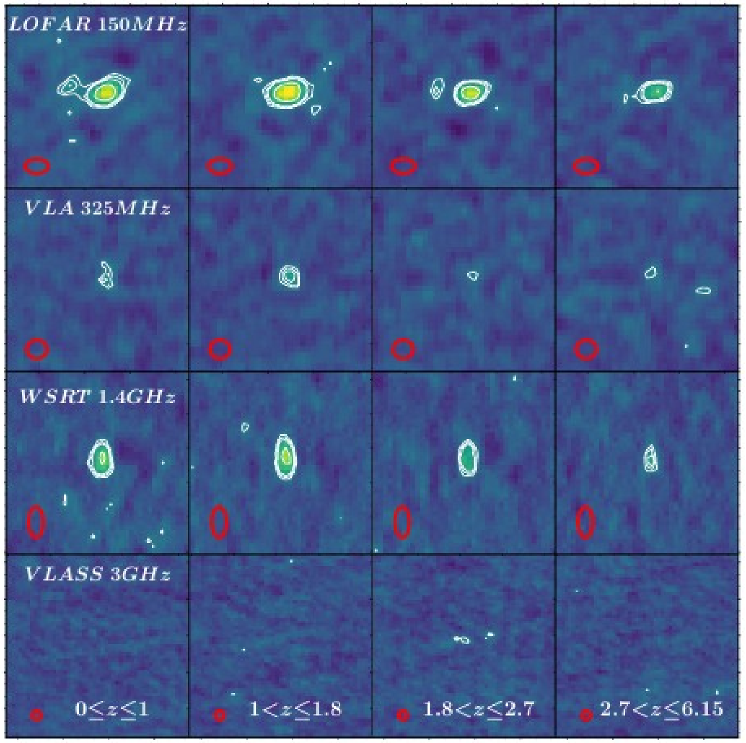

LOFAR Radio-undetected Quasars

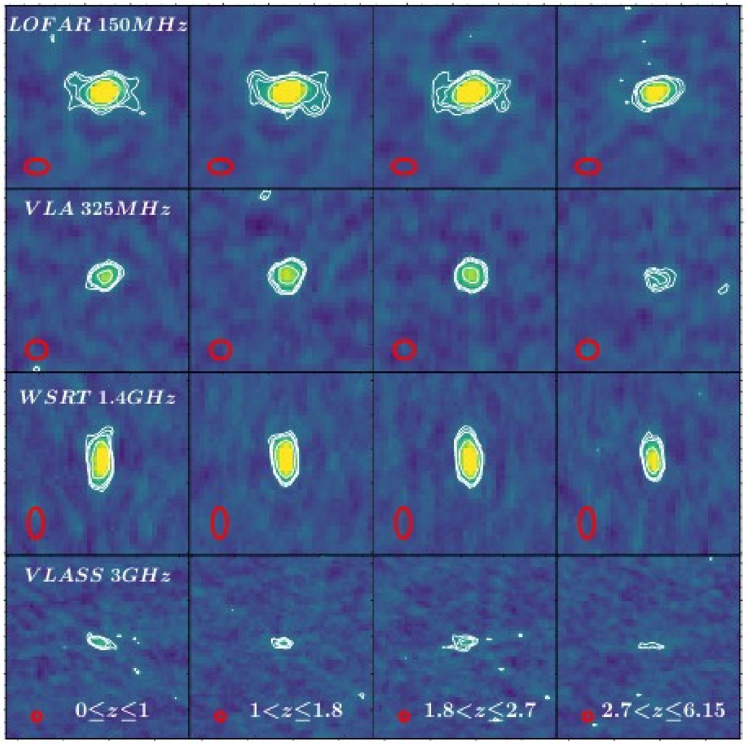

LOFAR Radio-detected Quasars

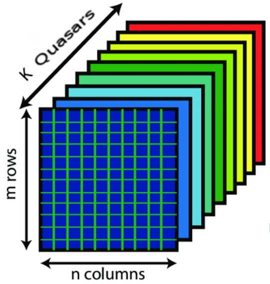

Image Stacking Results (Radio)

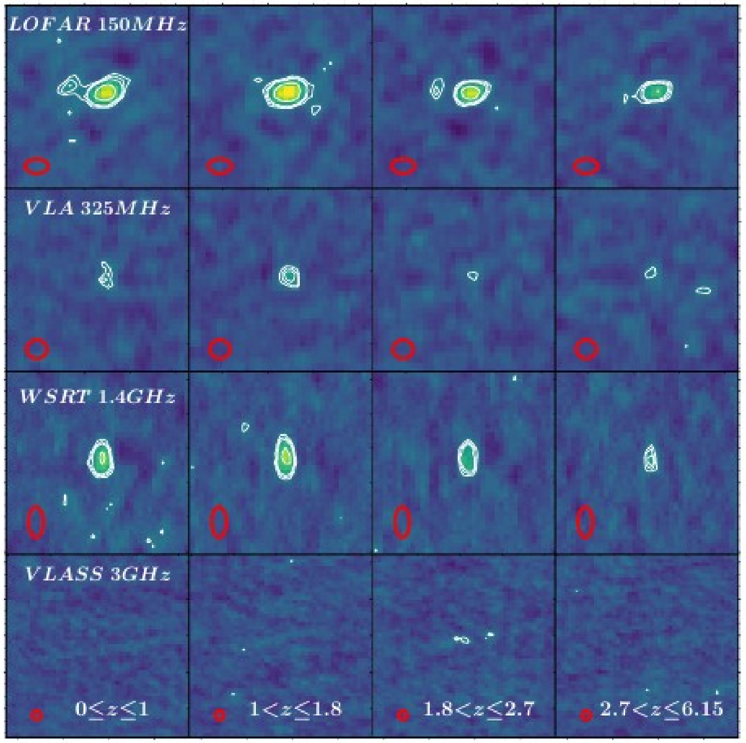

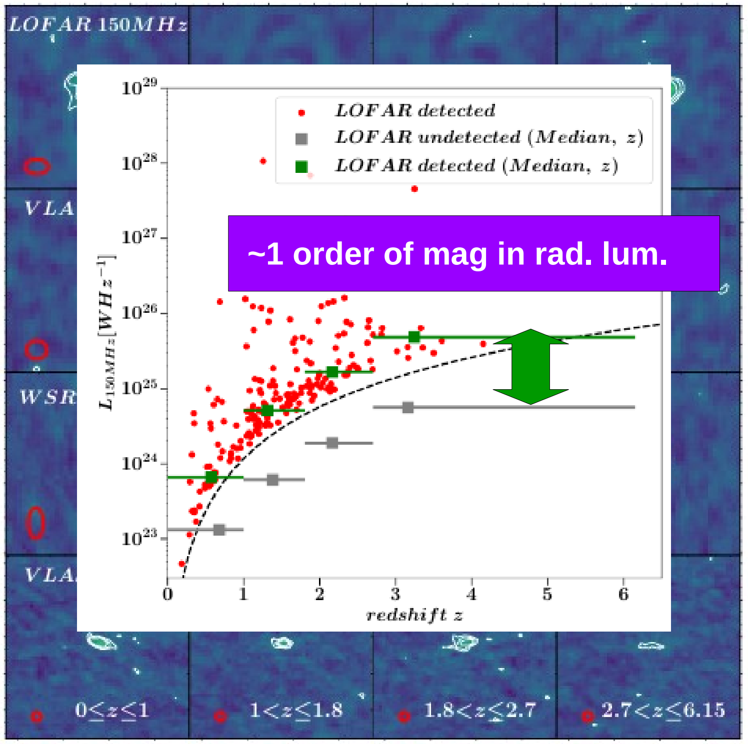

LOFAR Radio-Undetected Quasars

LOFAR Radio-Detected Quasars

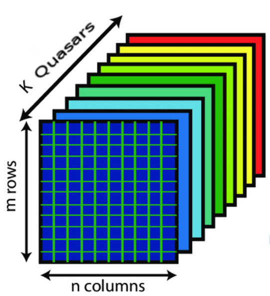

Retana-Montenegro et al. 2021 A&A, submitted.

Median Radio-Infrared Spectral Energy Distributions (SEDs)

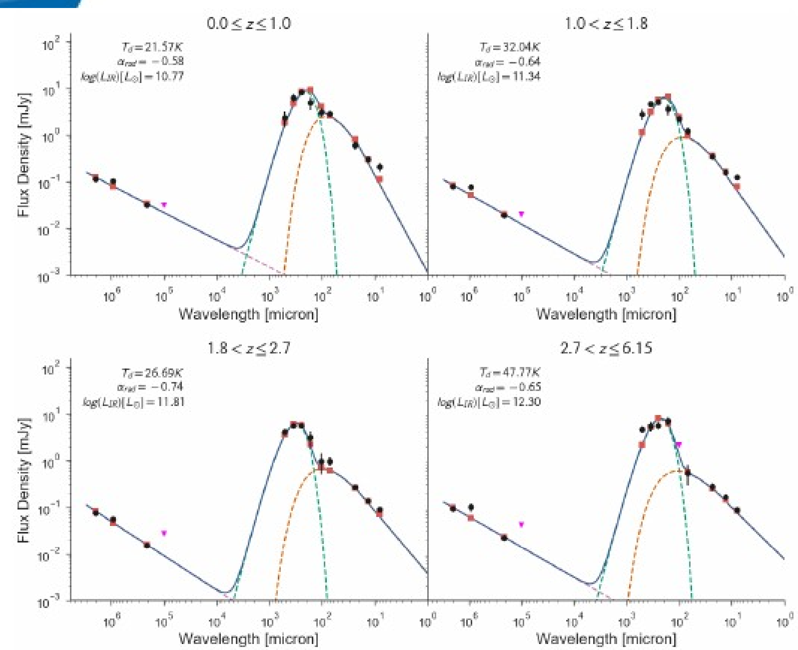

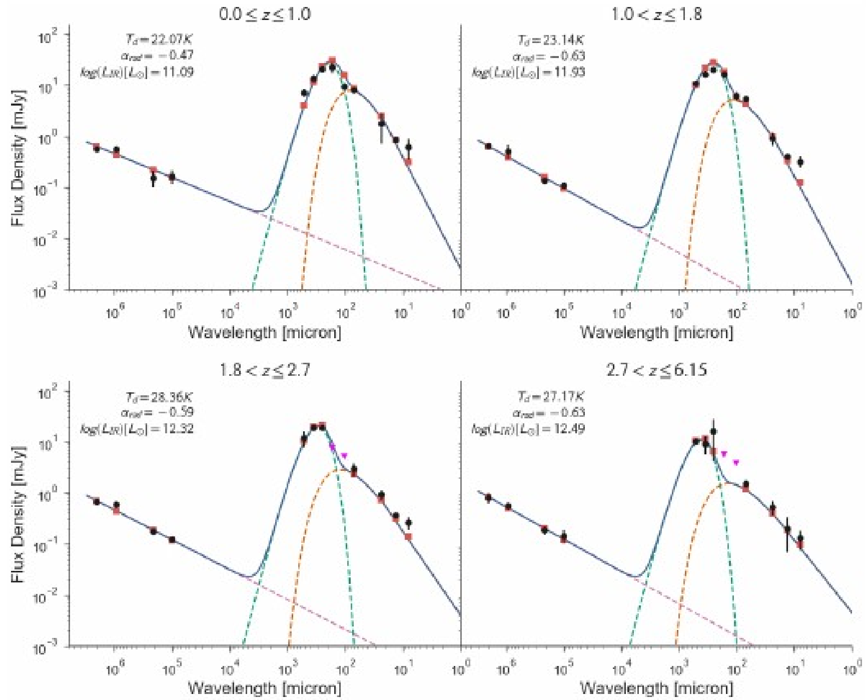

LOFAR Radio-Undetected Quasars

LOFAR Radio-Detected Quasars

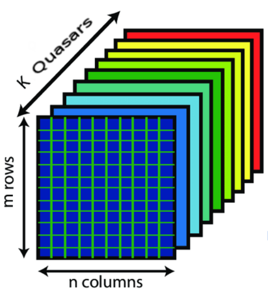

Three components: Power-law (Radio)+ Black Body+AGN (IR, Casey+12)

$$S_{\rm sync}(\lambda) = N_{\rm sync}\lambda^{\alpha}$$

$$S(\lambda) = N_{\rm AGN}\lambda^{\alpha_{\rm AGN}} e^{-(\lambda/\lambda_c)^2} + \frac{N_{\rm BB}}{e^{hc/\lambda kT}-1}\left(\frac{c}{\lambda}\right)^{\beta+3},$$

Far-Infrared Radio Correlation (FIRC)

$$q_{\rm FIR} = \log\left(\frac{L_{\rm IR}/3.75\times10^{12}\,{\rm Hz}}{L_{\rm Radio}}\right)$$

- Indicator widely used to investigate the levels of SF and AGN in galaxies (Helou+85, Bell+03, **Calistro-Rivera+17**).
- Gray region +/-2 FIRC.

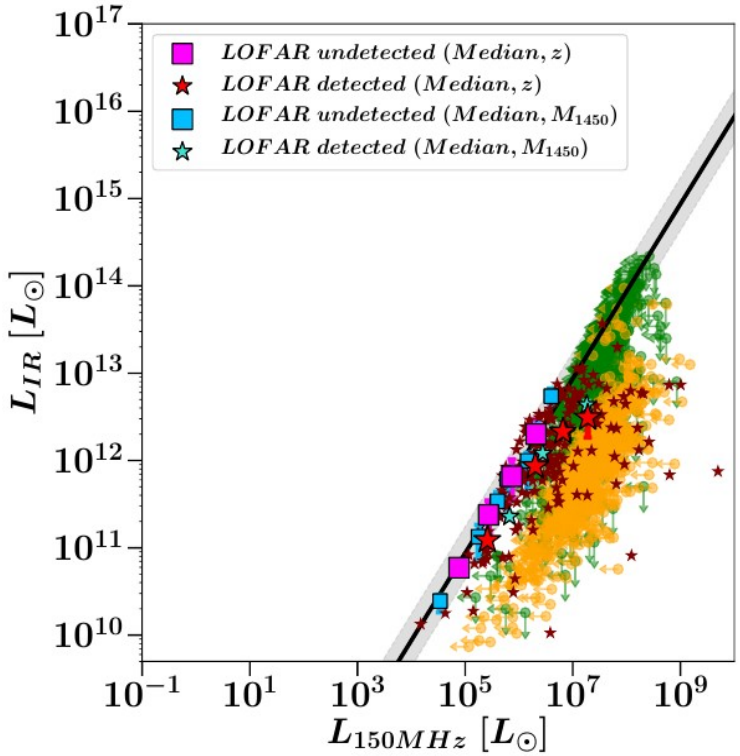

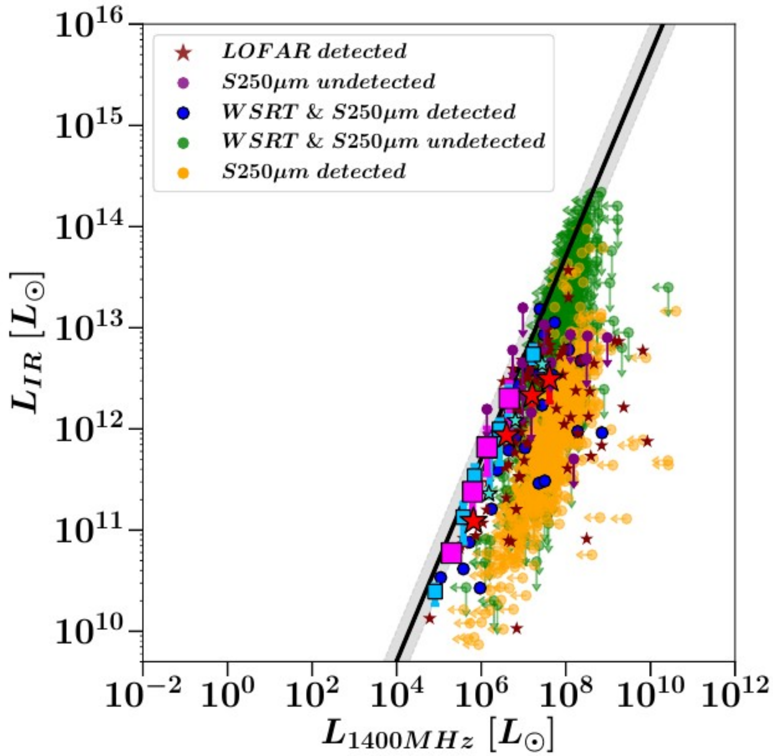

Retana-Montenegro et al. 2021 A&A, submitted.

Star-formation rates as function of luminosity

Optical Luminosity

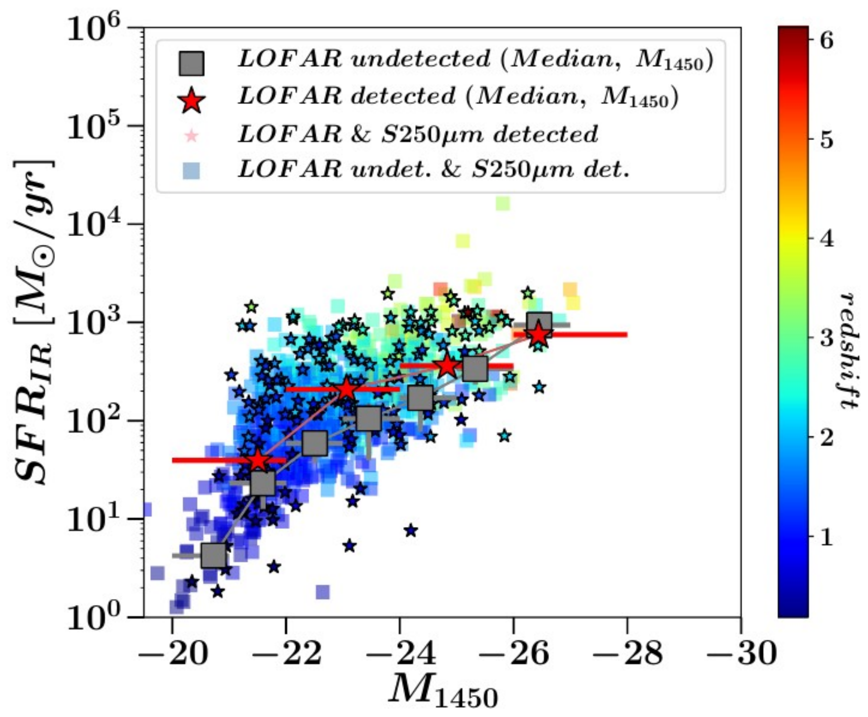

Retana-Montenegro et al. 2021 A&A, submitted.

Star-formation rates as function of luminosity

Optical Luminosity

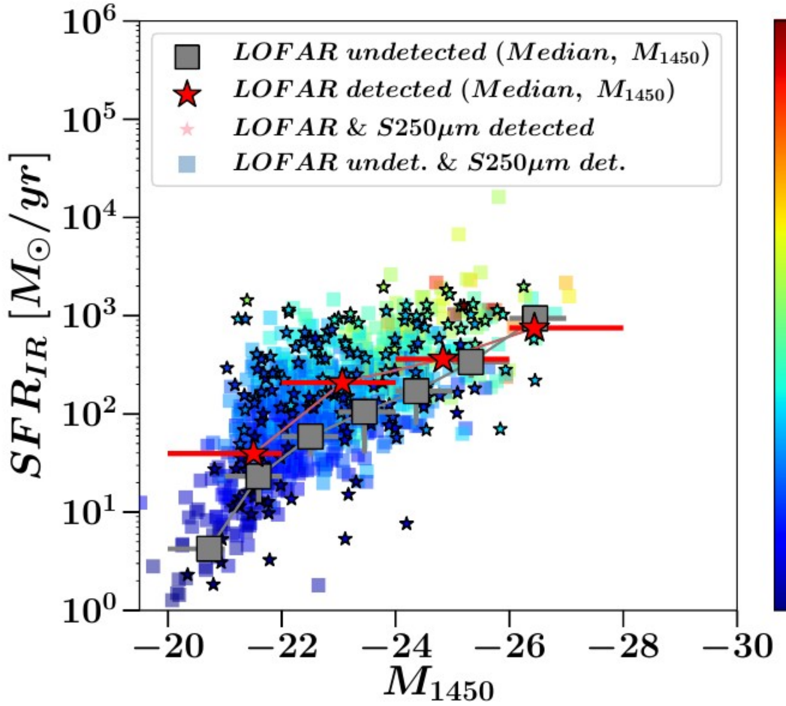

150MHz Radio Luminosity

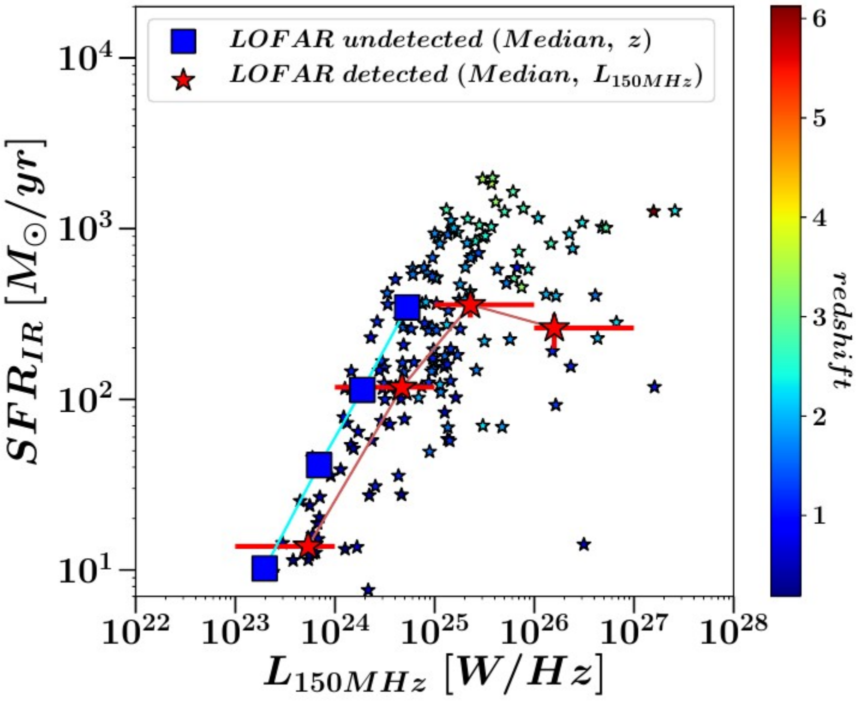

Retana-Montenegro et al. 2021 A&A, submitted.

Radio-loudness parameter

$$R = \log_{10}\left(\frac{L_{\rm rad}}{L_{\rm AGN}}\right)$$

Ratio of radio to infrared AGN luminoisity (Kellerman+89)

- Vertical dashed lines : Previous criteria used to classify quasars as RQQs or RLQs.

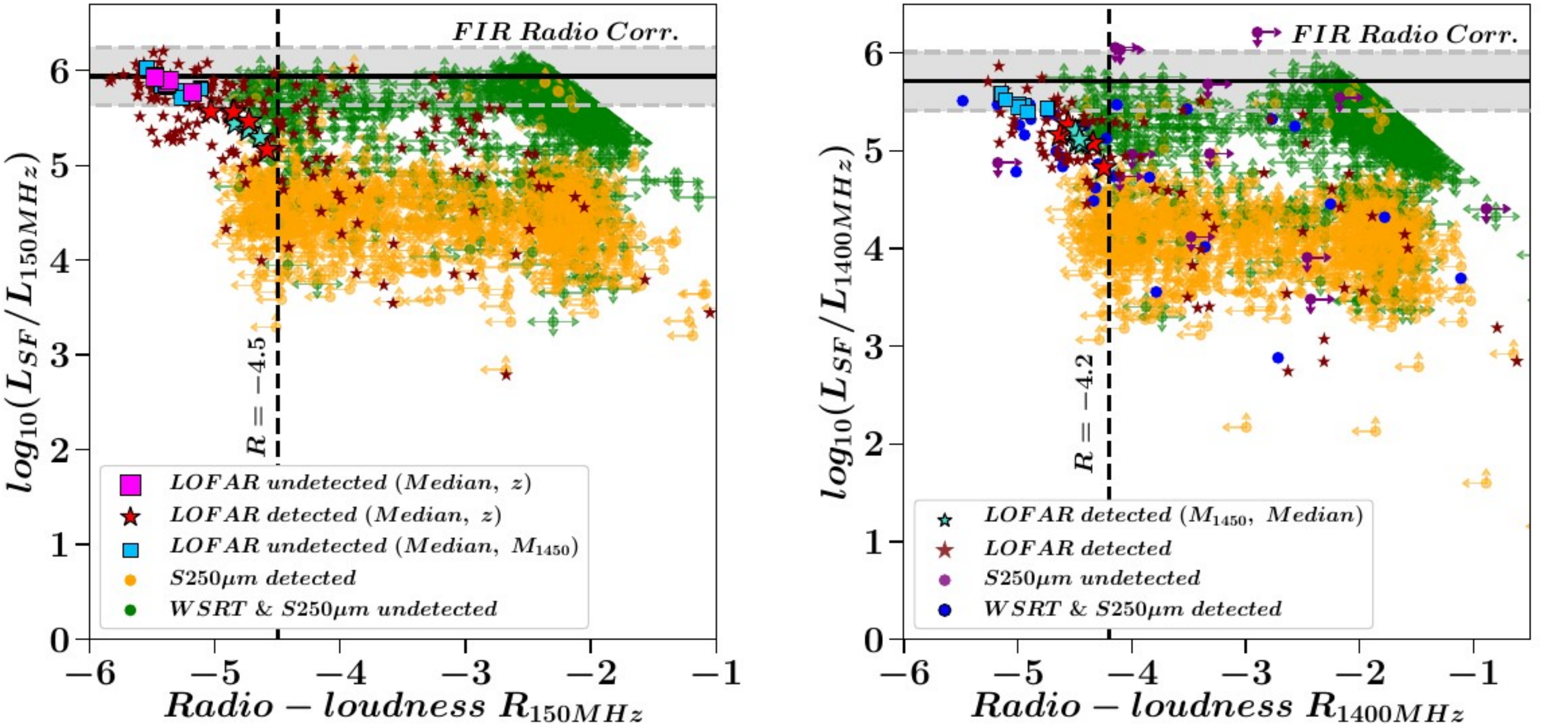

Retana-Montenegro et al. 2021 A&A, submitted.

Radio-loudness parameter

$$R = \log_{10}\left(\frac{L_{\rm rad}}{L_{\rm AGN}}\right)$$

Ratio of radio to infrared AGN luminoisity (Kellerman+89)

- Vertical dashed lines : Previous criteria used to classify quasars as RQQs or RLQs.

Weaker Radio Luminosity

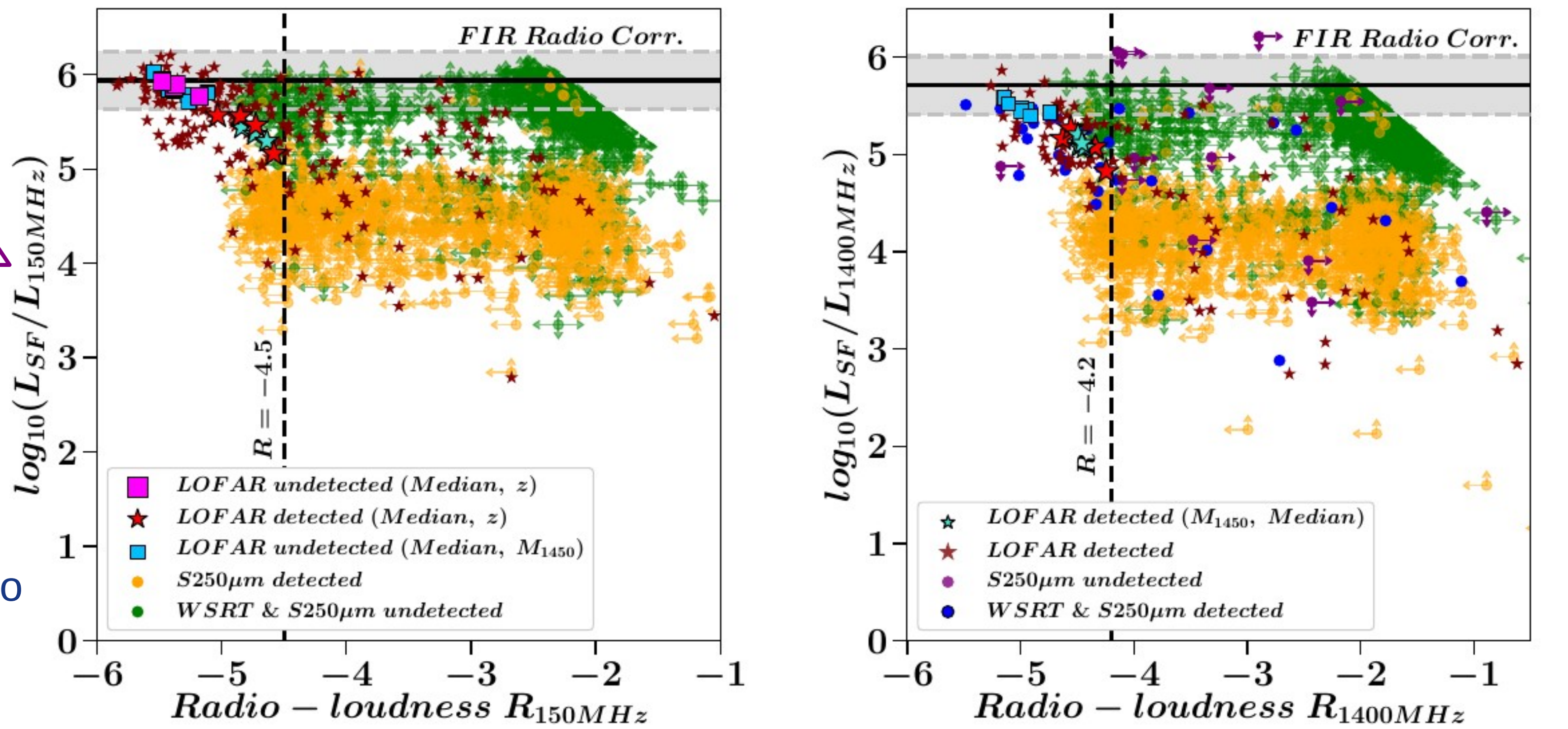

Jet Radio Power

Retana-Montenegro et al. 2021 A&A, submitted.

Radio-loudness parameter

$$R = \log_{10}\left(\frac{L_{\rm rad}}{L_{\rm AGN}}\right)$$

Ratio of radio to infrared AGN luminoisity (Kellerman+89)

- Vertical dashed lines : Previous criteria used to classify quasars as RQQs or RLQs.

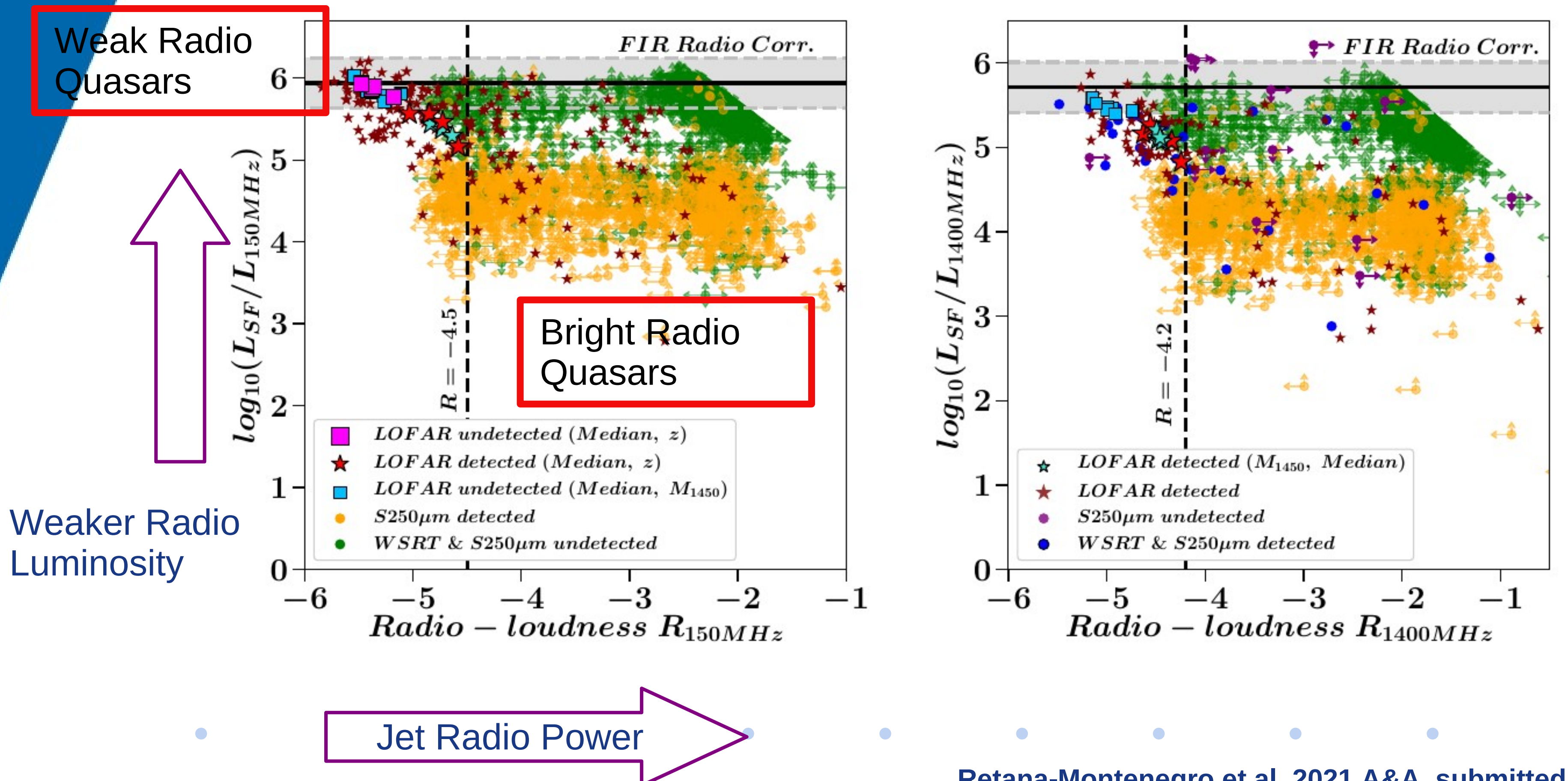

Retana-Montenegro et al. 2021 A&A, submitted.

Radio-loudness parameter

$$R = \log_{10}\left(\frac{L_{\rm rad}}{L_{\rm AGN}}\right)$$

Ratio of radio to infrared AGN luminoisity (Kellerman+89)

- Vertical dashed lines : Previous criteria used to classify quasars as RQQs or RLQs.

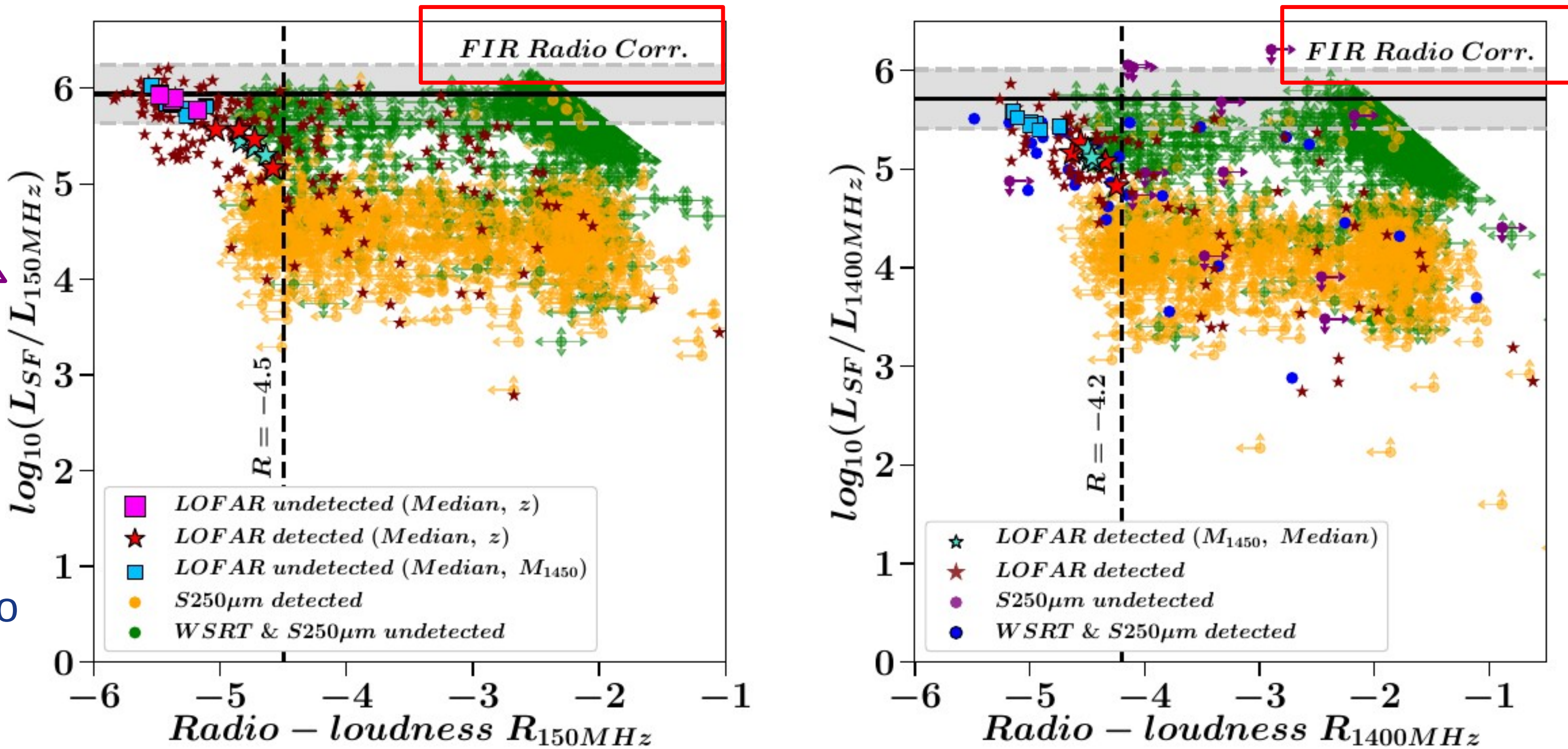

Weaker Radio Luminosity

Jet Radio Power

Retana-Montenegro et al. 2021 A&A, submitted.

Origins of radio-emission in radio-undetected quasars: a dominant mechanism or complex interplay?

$$L_{150\mathrm{MHz,\ acc}} = L_{150\mathrm{MHz}} - L_{150\mathrm{MHz,\ SF}}$$

150MHz Radio Luminosity associated to SMBH accretion

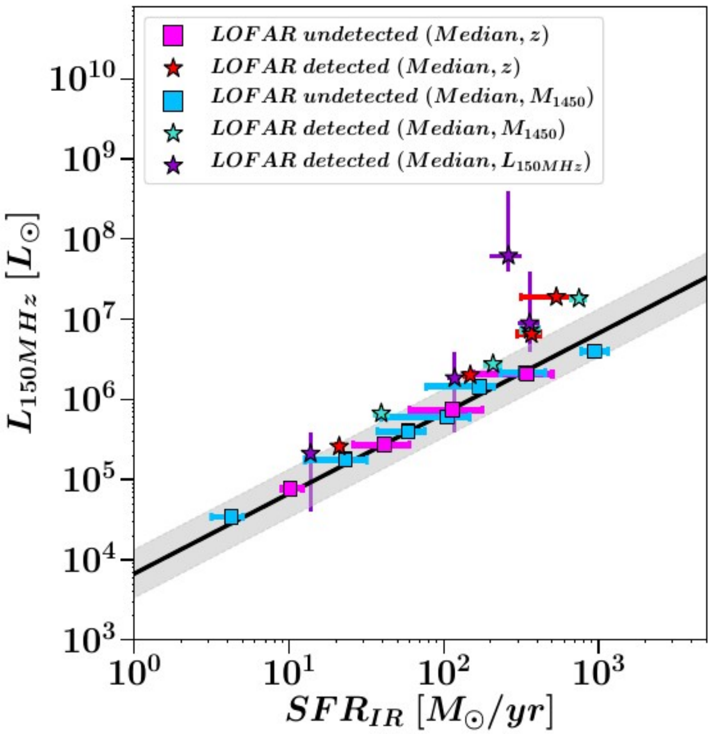

Retana-Montenegro et al. 2021 A&A, submitted.

Origins of radio-emission in radio-undetected quasars: a dominant mechanism or complex interplay?

$$L_{150\mathrm{MHz,\ acc}} = L_{150\mathrm{MHz}} - L_{150\mathrm{MHz,\ SF}}$$

150MHz Radio Luminosity associated to SMBH accretion

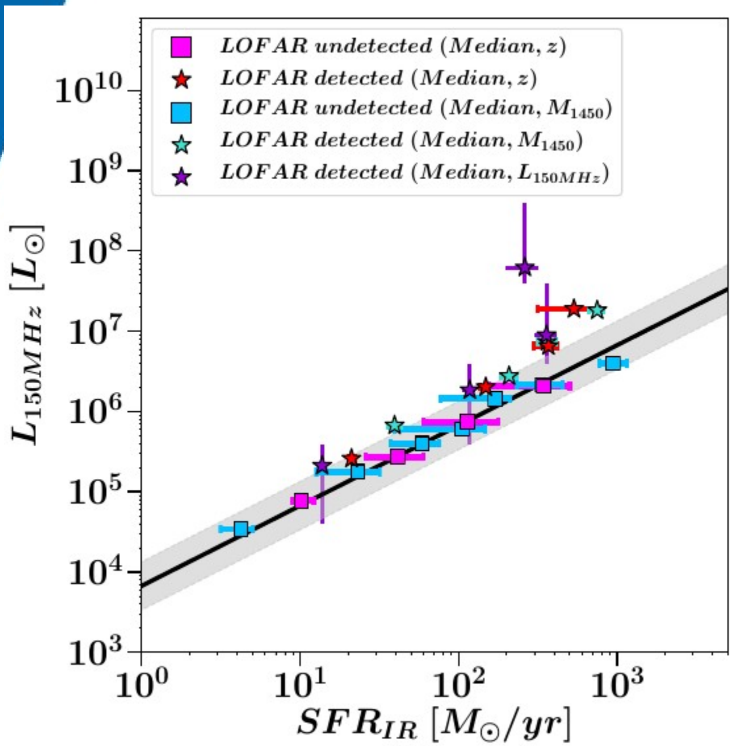

AGN negative Feedback?

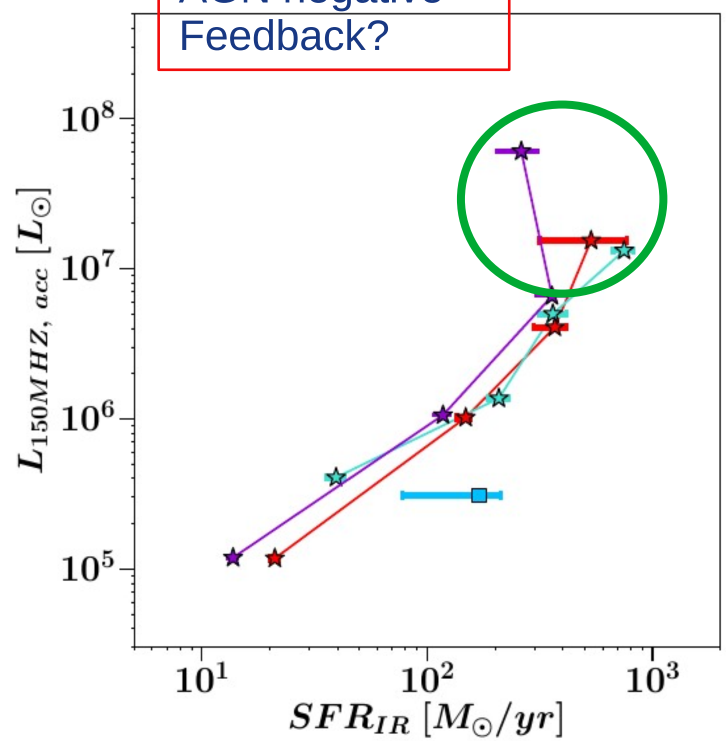

Retana-Montenegro et al. 2021 A&A, submitted.

- Vertica dashed lines : Previous criterium to classify quasars as RQQs or RLQs.

Origins of radio-emission in radio-undetected quasars: a dominant mechanism or complex interplay?

$$L_{150\mathrm{MHz,\ acc}} = L_{150\mathrm{MHz}} - L_{150\mathrm{MHz,\ SF}}$$

150MHz Radio Luminosity associated to SMBH accretion

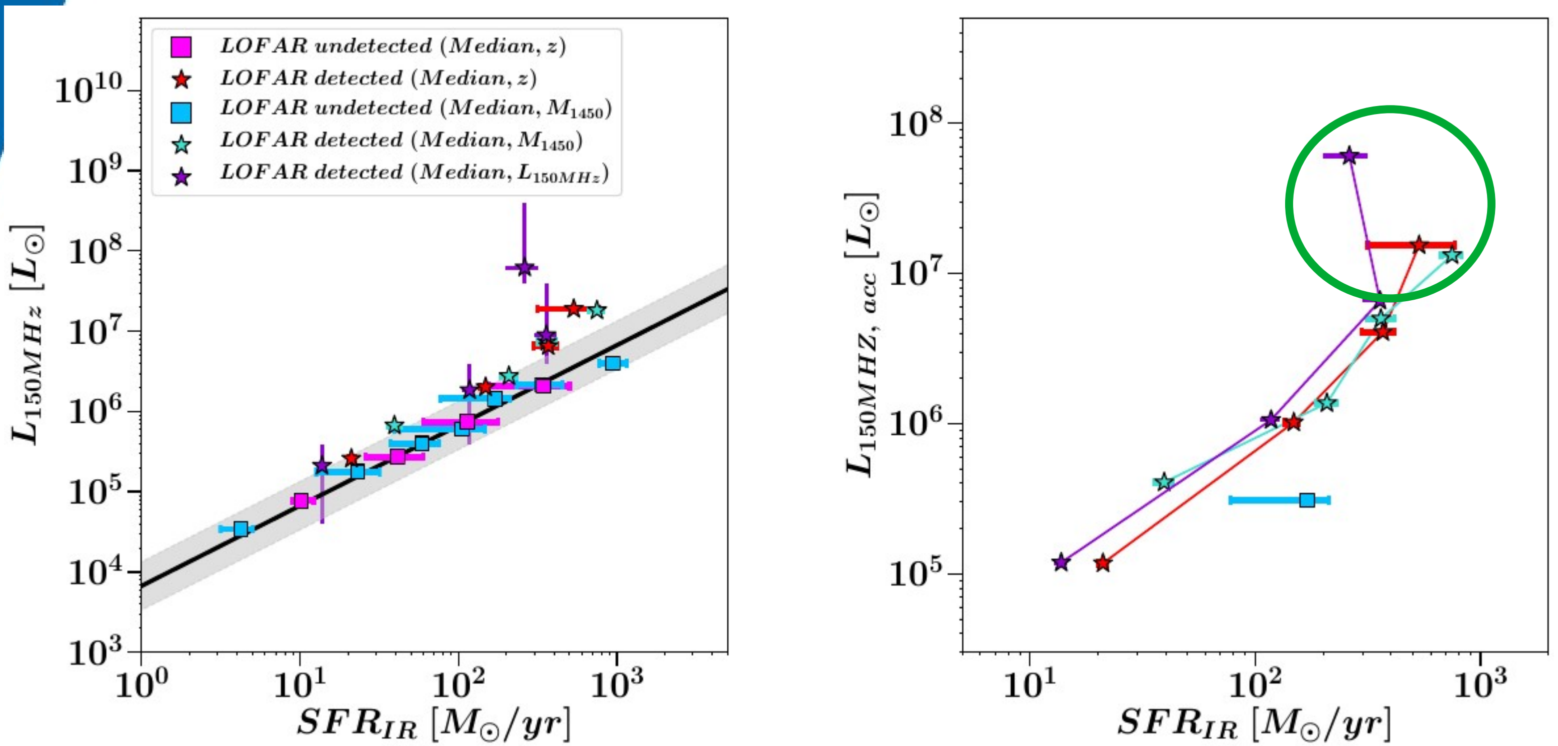

- RUQs have unphysical values at 150MHz. At 1.4GHz ~5-40%.
- RDQs stacked according to z and M1450: ~45-80%
- RDQs stacked according to L150: ~57-97%

Retana-Montenegro et al. 2021 A&A, submitted.

Take home message:

- RSQs present evolutionary trends that are *similar* to that of faint quasars (M_{1450}<-22).
- RSQs may compose to up ~20% of the total faint quasar population (M_{1450}<-22).
- Including a radio detection in the selection quasars helps to reduce stellar contamination.
- Stacking is power tool to study source populations that remain undetected even in deep radio surveys.
- Intense SF on the host galaxies of RDQs and RUQs
- Signatures of negative AGN feedback only in the most luminous RDQs, with radio-luminosity providing the best indicator.

Star-formation rates

- Two independent SFR estimates:
- IR (Kennicutt+98) and Radio (Condon+92; Yun+01)